Distribution Grid Voltage Support with Four Quadrant Control of Electric Vehicle Chargers

Jingyuan Wang[◇], Emin Y. Ucer[⊕], Sumit Paudyal[◇], Mithat C. Kisacikoglu[⊕], and Mohammad A. I. Khan[◇]
[◇]Michigan Technological University, USA; [⊕]The University of Alabama, USA.
Emails: jwang11@mtu.edu, eucer@crimson.ua.edu, sumitp@mtu.edu, mkisacik@ua.edu, mkhan22@mtu.edu

***Abstract*—Conventionally, voltage control in distribution grids has been achieved through load tap changers, capacitor banks, and network switches. With the advancements in on-board electric vehicle (EV) chargers, voltage control can be achieved through control of EV charging/discharging as EVs can operate in any of the four P-Q quadrants with slight modifications to the charger. In this work, we use a high-fidelity on-board EV charger model, which has been validated using actual measurements. Then, we coordinate the four quadrant operation of EVs and distribution feeder to support voltage control in the grid. The efficacy of the developed models are demonstrated by using an LV secondary feeder. Operation of EVs in all four quadrants are shown to compensate for the feeder voltage fluctuations caused by daily time varying residential loads, while satisfying operational constraints of the feeder.**

***Index Terms*—Electric vehicles, optimization, distribution grid, voltage control, reactive power control.**

I. Introduction

Electric vehicle (EV) production from progressive manufacturers is gradually going up as the technology is increasingly adopted by customers who care about environment and energy. EV charging will soon become part of our everyday life. The challenge following this trend is that EV charging stresses the electric power grid especially when the system is at peak load. Solutions to detrimental impacts (such as transformer overloading, voltage drop, power losses) of EVs need to be investigated. To give a perspective on the adverse impact, study shows that 45% EV penetration can cause 25% more power losses and 50% transformer overloading in distribution feeders [1].

One way to deal with peak load problems caused by EV charging is illustrated in [2], [3], which is unidirectional EV charging management. Another effective way is bidirectional vehicle-to-grid (V2G) technology which allows EV batteries to discharge active and reactive power into the grid [4]. V2G can help with reactive power compensation, voltage stability, peak shaving, etc [5]. Distribution System Operator (DSO) may be involved in this process to ensure feasibility of distribution grid operations. DSO may either limit EV charging base on peak loads [6], use optimization-based models which aim at minimizing power losses/operational costs [7], or maximizing benefits [8] to coordinate EV charging. Coordinated charging of EVs can help power grids to stay within grid operational constrains including the voltage profiles of the feeder [9], [10].

EVs can support ancillary services and demand response in power grid as they are flexible and schedulable loads [11]. Actually, EVs have great potential to help with both frequency regulation and voltage control problems in power grid as they can provide active/reactive power back to the grid [12]. At the distribution level, EVs can provide Volt/Var support [13]–[16]. Conventionally, Volt/Var control in distribution grids has been achieved through load tap changers (LTCs), shunt capacitors, and network switches. Since EVs can operate in any of the four quadrants of P-Q coordinate system, EVs have the ability to effectively consume/provide reactive power locally, and without impacting life cycles of the batteries [12].

Studies on reactive power support from EVs and its implementation are limited in literature. Voltage regulation with EVs and LTCs in distribution grids is discussed in [17]. Four-quadrant P-Q control of EV charging to control voltages in distribution grids is discussed in [18], [19]. Although these studies showed role of reactive power support from EVs to the grid, they are mainly focused on modeling from grid side while EV charger models are overly simplified.

In this work, we use a high-fidelity EV battery charger model, which has been validated using actual measurements, and then, we coordinate the four quadrant operations of EVs and distribution feeder to support voltage control on the grid. In the proposed coordinated framework, EVs send their preferences and parameters (such as power rating, SOC, etc.) to the DSO. Then, DSO solves an optimal power flow (OPF) model at the grid level and generates voltage regulation signals that each EVs are recommended to follow. The main contributions of the paper are: *a)* development and validation of detailed high-fidelity EV charger and battery models for 4-quadrant operations, and *b)* integration of the EV charger/battery model to grid optimization model for voltage control applications.

II. EV Charger Model and Validation

In this study, we developed a new on-board charger and battery system model as illustrated in Fig. 1. The model consists of both AC and DC system dynamics of an EV. The model has two sections: i) AC grid connection and ii) DC battery model. It employs constant current (CC)/constant voltage (CV) control of the DC battery charging current. Furthermore, a second-order transfer function of AC system response of the on-board charger is used. This is based on experimentally collected data from Toyota IQ EV [20].

The battery cell model consists of an open-circuit cell voltage in series with an equivalent internal resistance. Both the equivalent resistance (R_{eq}) and the open-circuit voltage (OCV) are a function of the battery SOC as described as a function in Fig. 2. In this study, a 24.8 Ah, 3.7 V nominal, baseline Li-on battery cell is used to form the battery pack model for each EV. The EVs are formed in three categories with respect to their battery energy capacities, i.e. short (8 kWh), medium (15 kWh), and long (30 kWh) electric-only range. Various cell configurations are used to meet the

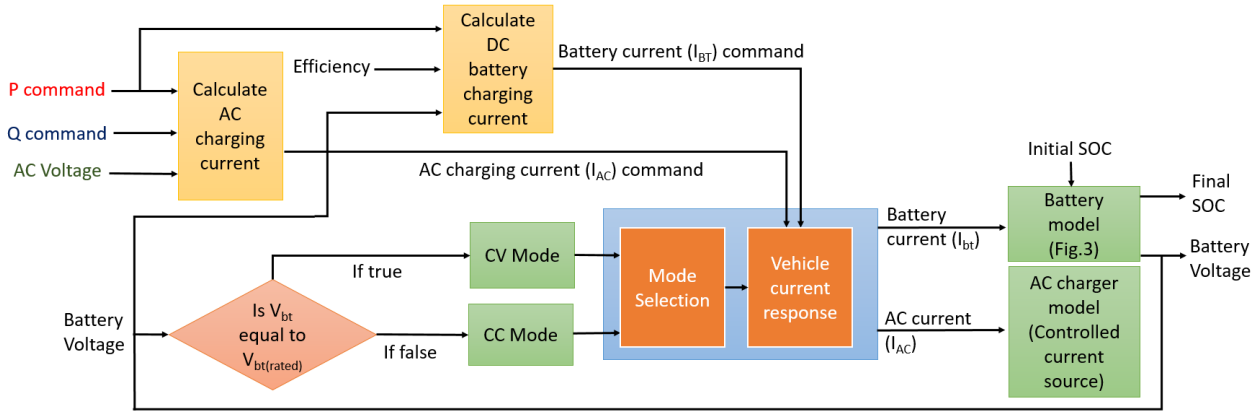

Fig. 1: High-level overview of the battery model for active/reactive power control of EVs.

nameplate battery energy capacity. This cell model can capture the impact of battery SOC calculation on the performance of the developed charging algorithm which is in the scale of minutes.

The battery cell voltage is an important indicator to determine when to switch from CC to CV charging. Here, when the cell voltage reaches 4.0 V, the charge cycle switches to CV charging. The battery cells are assumed to be equally charged with proper equalization by the battery management system.

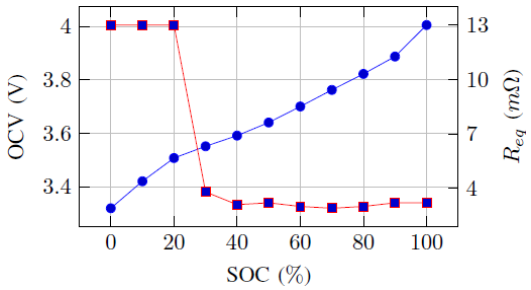

Fig. 2: Li-ion cell characteristics used for modeling battery systems: cell voltage vs. SOC (circle, blue) and equivalent resistance vs. SOC (square, red).

In CC mode, the DC battery current (I_{bt}) is controlled by the commanded active power (P^{ev}). When switched to CV mode, the battery current is exponentially reduced while keeping the battery voltage constant at a maximum value.

The vehicle AC current response is modeled using a second order transfer function, whose parameters are obtained from experimental data [20]. The on-board charger is also limited by a rate-limiter. The calculated approximate ramp-rate of the controller is 5.35 A/s. This is a non-linear check of the current ramp that is embedded within the controller. The minimum accepted rms reference current command is 0 A and the maximum is 14 A as modeled using a saturation block.

The mathematical model of the battery is implemented using Simulink. The EVs are operated in four quadrants based on arbitrary P,Q set points sent to the EVs for 60 minutes. The set points are limited between -3.3 to 3.3 kVA (which is the rated capacity of the battery). Fig. 3, Fig. 4, and Fig. 5 show response of the battery in terms of active power tracking, reactive power tracking, and SOC dynamics, respectively. The model features essential charging dynamics of an on-board charger and an EV battery. It is capable of tracking active and reactive power commands given by the DSO.

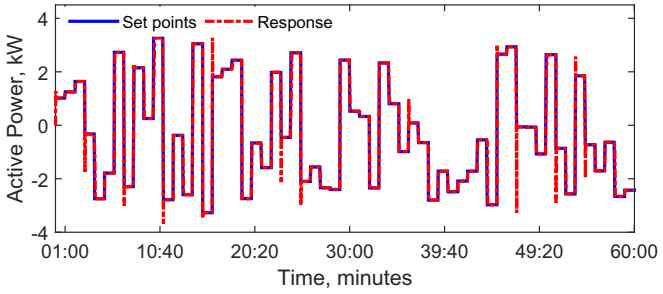

Fig. 3: Response of battery for active power set points.

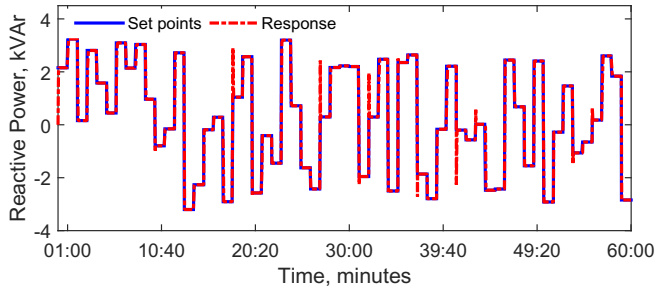

Fig. 4: Response of battery for reactive power set points.

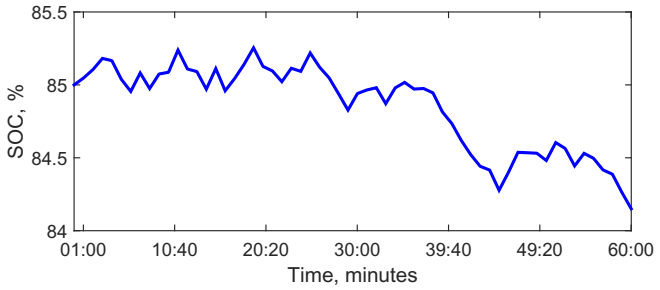

Fig. 5: SOC as battery model tracks dynamic set points.

III. Optimal Voltage Regulation Model

We have extended prior work on distribution optimal power flow (DOPF) model in [21] to create voltage regulation signals

(in terms of active power and reactive power dispatch of EVs) from the DSO's point of view. The DOPF model is built using individual grid components and circuit laws. The mathematical models are developed in terms of branch current and nodal voltages. The conductors and cables are modeled using π-equivalent circuits. Detailed descriptions of these models can be found in [21].

$$\textbf{Min:}\quad \Phi = \sum_{\mathbf{m}\in\mathbf{N},\,\mathbf{t}\in\mathbf{T}} \left(\mathbf{V_{m,t}} - \mathbf{V^{min}}\right)^2 \tag{1}$$

subject to:

(Grid Level Constraints)

$$\mathbf{V_{j,t}} = \sum_{\mathbf{k}\in\mathbf{N}} \mathbf{Y_{j,k}}\,\mathbf{I_{k,t}} \quad \forall\, \mathbf{j}\in\mathbf{N}, \mathbf{t}\in\mathbf{T} \tag{2}$$

$$\mathbf{P^{ev}_{j,t}} + \mathbf{P^{L}_{j,t}} = \mathbf{Real}\left(\mathbf{V_{j,t}}\,\mathbf{I^{*}_{j,t}}\right) \quad \forall\, \mathbf{j}\in\mathbf{N}, \mathbf{t}\in\mathbf{T} \tag{3}$$

$$\mathbf{Q^{ev}_{j,t}} + \mathbf{Q^{L}_{j,t}} = \mathbf{Imag}\left(\mathbf{V_{j,t}}\,\mathbf{I^{*}_{j,t}}\right) \quad \forall\, \mathbf{j}\in\mathbf{N}, \mathbf{t}\in\mathbf{T} \tag{4}$$

$$\mathbf{V^{min}} \le \mathbf{V_{m,t}} \le \mathbf{V^{max}} \quad \forall\, \mathbf{m}\in\mathbf{N}, \mathbf{t}\in\mathbf{T} \tag{5}$$

(EV Level Constraints)

$$\mathbf{P^{ev}_{m,t}} = \mathbf{u^{c}_{m,t}}\,\mathbf{P^{c}_{m,t}}\,(\eta_{|\mathbf{m,t}})^{-1} - \mathbf{u^{d}_{m,t}}\,\mathbf{P^{d}_{m,t}}\,\eta_{|\mathbf{m,t}} \quad \forall\, \mathbf{m}\in\mathbf{N}, \mathbf{t}\in\mathbf{T} \tag{6}$$

$$\mathbf{Q^{ev}_{m,t}} \le \sqrt{\left(\mathbf{R^{ev}_{m,t}}\right)^2 - \left(\mathbf{P^{ev}_{m,t}}\right)^2} \quad \forall\, \mathbf{m}\in\mathbf{N}, \mathbf{t}\in\mathbf{T} \tag{7}$$

$$\mathbf{Q^{ev}_{m,t}} \ge -\sqrt{\left(\mathbf{R^{ev}_{m,t}}\right)^2 - \left(\mathbf{P^{ev}_{m,t}}\right)^2} \quad \forall\, \mathbf{m}\in\mathbf{N}, \mathbf{t}\in\mathbf{T} \tag{8}$$

$$\mathbf{s^{ev}_{m,t}} = \mathbf{s^{ev}_{m,t-1}} + \Delta\mathbf{t}\,(\mathbf{E^{cap}})^{-1}\left(\mathbf{u^{c}_{m,t}}\,\mathbf{P^{c}_{m,t}}\,(\eta_{|\mathbf{m,t}})^{-1} - \mathbf{u^{d}_{m,t}}\,\mathbf{P^{d}_{m,t}}\,\eta_{|\mathbf{m,t}}\right) \quad \forall\, \mathbf{m}\in\mathbf{N}, \mathbf{t}\in\mathbf{T} \tag{9}$$

$$\mathbf{s^{ev}_{m,t}} = \mathbf{s^{ev}_{m,0}} + \Delta\mathbf{t}\,(\mathbf{E^{cap}})^{-1}\left(\mathbf{u^{c}_{m,t}}\,\mathbf{P^{c}_{m,t}}\,(\eta_{|\mathbf{m,t}})^{-1} - \mathbf{u^{d}_{m,t}}\,\mathbf{P^{d}_{m,t}}\,\eta_{|\mathbf{m,t}}\right) \quad \forall\, \mathbf{m}\in\mathbf{N}, \mathbf{t}=\mathbf{1} \tag{10}$$

$$\mathbf{s^{min}} \le \mathbf{s_{m,t}} \le \mathbf{s^{max}} \quad \forall\, \mathbf{m}\in\mathbf{N}, \mathbf{t}\in\mathbf{T} \tag{11}$$

$$\mathbf{u^{c}_{m,t}} + \mathbf{u^{d}_{m,t}} \le \mathbf{1} \quad \forall\, \mathbf{m}\in\mathbf{N}, \mathbf{t}\in\mathbf{T} \tag{12}$$

$$\mathbf{u^{c}_{m,t}}, \mathbf{u^{d}_{m,t}} \in \{\mathbf{0},\mathbf{1}\} \quad \forall\, \mathbf{m}\in\mathbf{N}, \mathbf{t}\in\mathbf{T} \tag{13}$$

In the above formulation, $\Delta\mathbf{t}$ represents time interval, η represents EV's efficiency, Φ represents objective function value, $\mathbf{E^{cap}}$ represents battery capacity, $\mathbf{I}$ is nodal current injection, $\mathbf{j},\mathbf{k}\in\mathbf{N}$ represent EV number, $\mathbf{m}\in\mathbf{N}$ is set of nodes with EVs and loads, $\mathbf{P^{c}}$ is EV charging power, $\mathbf{P^{d}}$ is EV discharging power, $\mathbf{P^{ev}}$ is EV power on grid side, $\mathbf{P^{L}}$ is active power of load, $\mathbf{Q^{ev}}$ is reactive power of EV on grid side, $\mathbf{Q^{L}}$ is reactive power of load, $\mathbf{R^{ev}}$ is charger rating, $\mathbf{s_0}$ is initial SOC, $\mathbf{s^{ev}}$ is battery SOC, $\mathbf{s^{max}}$ is maximum SOC, $\mathbf{s^{min}}$ is minimum SOC, $\mathbf{t}\in\mathbf{T}$ is time index, $\mathbf{u^{c}},\mathbf{u^{d}}$ charging/discharging status of EV, $\mathbf{V}$ is nodal voltage, $\mathbf{V^{max}}$ is maximum nodal voltage limit, $\mathbf{V^{min}}$ is minimum nodal voltage limit, and $\mathbf{Y}$ is Y-bus matrix.

Equation (1) minimizes the voltage deviation from minimum allowed limit at EV nodes. This objective function ensures EVs get opportunity to charge when the base load is not causing excessive voltage drop issue (i,e., EVs operate in I and IV P-Q quadrants). At times, when voltage with base load goes below the minimum limit, the objective function will also force EV to discharge (i.e., EVs operate in II and III P-Q quadrants). Equation (2) represents the network model. Equations (3) and (4) represent the load models. Equation (5) ensures the nodal voltage limits. Equation (6) represents EV power in terms of charging and discharging powers. Equations (7) and (8) calculate and bound the reactive power of EVs based on socket KVA rating and EVs' active power. Equation (9) and (10) represent SOC dynamics, and (11) represents SOC limits. Equations (12) ensures charging and discharging would not take place simultaneously, and (13) ensures the binary values on charging/discharging decision. This model is non-linear mixed integer in nature, and the variables $\mathbf{P^{ev}_{m,t}}$ and $\mathbf{Q^{ev}_{m,t}}$ represent the dispatch signals send to EVs in order to maintain voltage profile on the feeder. Note that the regulation signals are not binding in the proposed model, as the reactive power capability depends on active power of the battery, and active power tracking is given priority over reactive power tracking. The proposed model tries to track the voltage regulation signals as closely as possible.

IV. Case Studies

The 240 V lateral in [22] is modified for the case studies in this paper. As Fig. 6 shows, a 175 kVA, 14.4/0.24 kV transformer is feeder the circuit. The impedance of the transformer is $0.0143+\mathrm{j}0.0357\Omega$ on the low voltage side. 24 houses are supplied by this feeder and impedance of every lateral branch (e.g., 52-53) and vertical branch (e.g., 52-1) are $0.0069+\mathrm{j}\,0.0018\Omega$ and $0.011+\mathrm{j}\,0.0017\Omega$ respectively. EV model and grid model are built in Simulink and solved with ePHASORSIM solver. Voltage regulation model is built in GAMS and solved using KNITRO solver. The power consumption profile of 24 houses in a summer day is shown in Fig. 7. Fig. 8 shows the voltage profiles for selective houses (House 8, 16, 24) and it indicates that the feeder has undervoltage issue when the load is at peak. We deploy EVs having communication capabilities to the DSO or the aggregator, and we assume that initial SOC are readily available when EVs connect to the grid. This is not a strong

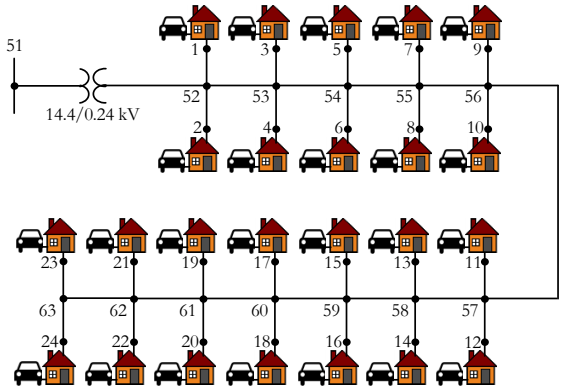

Fig. 6: LV 240V Feeder with 24-houses used for the studies.

assumption, given new IEE 1547 standard [23] requires that all DERs must be equipped with communication capabilities.

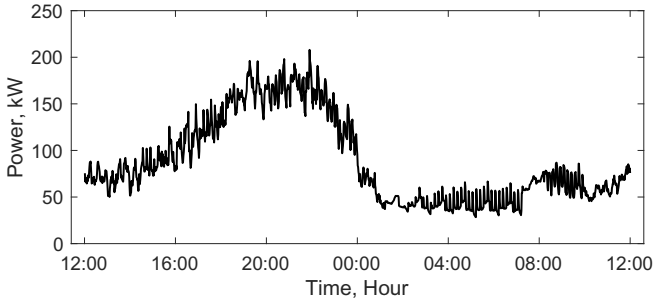

Fig. 7: Base load profile on the feeder.

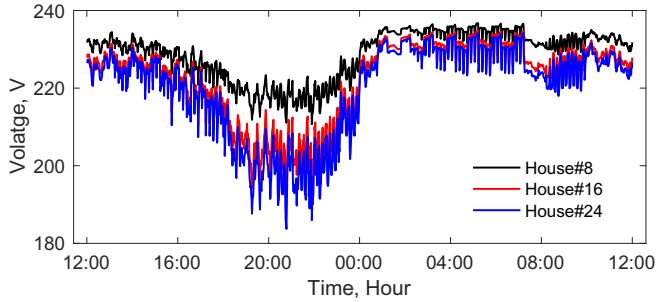

Fig. 8: Voltage profile at selective houses (8,16,and 24).

Next, we show two case studies to demonstrate effective use of reactive power and four-quadrant P-Q operation of EV chargers for voltage support applications.

Case-A: Due to limited battery capability and arrival/ departure pattern, EVs may not be always available to provide support to grids. Thus, case studies are carried out by considering one hour block (00:00 and 1:00 AM) when EVs are grid connected. The time is chosen such that the base load is low. This ensures voltage drop is not significant and the available voltage margins allow EVs to charge. For comparative analysis, we dispatch EVs with and without reactive power.

Voltage profiles at House-24 with base load and with EV loads are shown in Fig. 9. Since EV is charging, battery SOC is increasing (see Fig. 10), while reactive power dispatch is mostly positive as well. As EV is in charging mode for the selected hour, voltage profile is low compared to the base case. We observed that upstream EVs, which are closer to

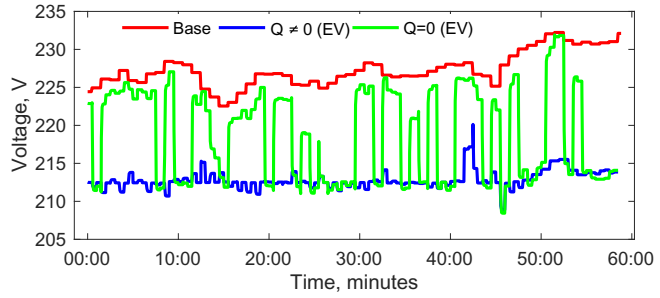

Fig. 9: Voltage profile at House-24 with base, with EV loads (Q = 0 and Q $\neq$ 0).

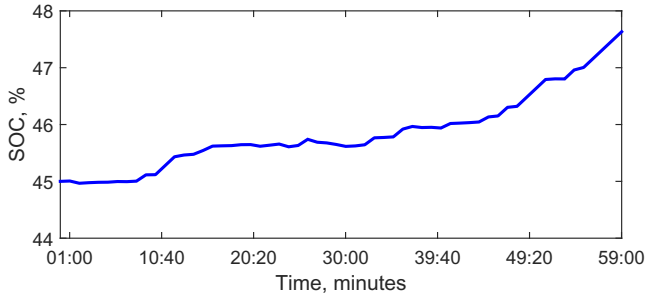

Fig. 10: SOC dynamics of EV battery at House 24 when the base load is low (EV is effectively charging).

the service transformer, has more voltage room to charge than downstream EVs. Therefore, the optimal voltage regulation signal provides higher active power set points to upstream EVs. During the EV charging, the voltage profile of House-24, which is the farthest node from the transformer becomes limiting as it hits the lower prescribed limit first.

Case-B: This case demonstrates how 4-quadrant operation of EVs help support voltage profile in the feeder. Simulation is carried out for one hour between 10:00 to 11:00 PM, when the base load is at peak and EVs are home. Voltages profile with base load are mostly below statutory limits; therefore, voltage regulation signal from DSO forces most of the EVs to discharge and provide power back to the grid. However, some EVs may still operating in the charging mode since EVs have different arrival and departure pattern/SOC and are connected on nodes with different voltage profiles. Voltage profiles at House-24 with and without EVs are shown in Fig. 11. Simulation includes EVs operating in unity power factor and with reactive power dispatch. With reactive power support from EV, we observed that the voltage fluctuations can be smoothen.

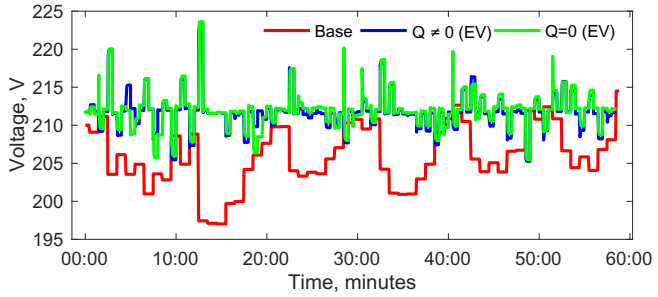

Fig. 11: Voltage profile at House 24 with base load and EVs (Q = 0 and Q $\neq$ 0).

Response of active power dispatch of battery in tracking optimal voltage regulation signal is shown in Fig. 12. Since the rating of charger is 3.3 kVA, tracking is not prefect in Fig. 12 as some of the capacity is used for the reactive power tracking as well in the 4-quadrant mode. Response of the battery in tracking reactive power set point is shown in Fig. 13. The case studies clearly demonstrate the effective use of 4-quadrant EV charging for voltage support on LV feeder.

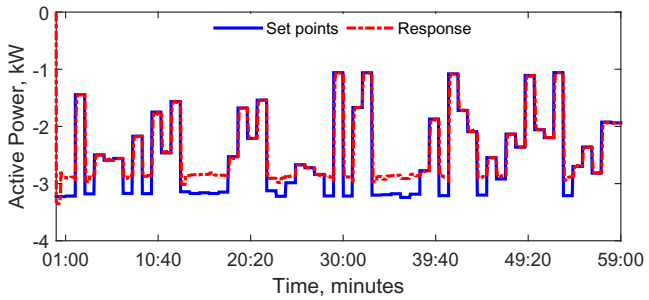

Fig. 12: Response of active power of EVs at House 24 when reactive power is not zero (peak load).

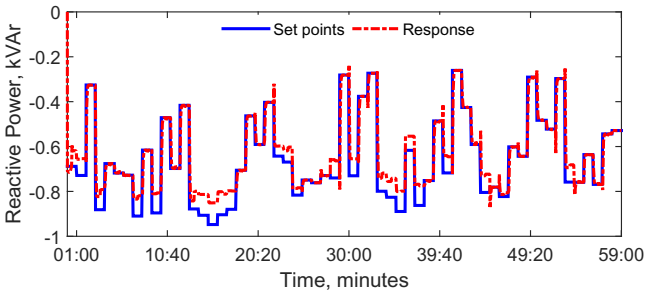

Fig. 13: Response of reactive power of EVs at House 24 when reactive power is not zero (peak load).

Note that this paper discussed the benefits of reactive power dispatch of EVs from DSO's perspective. However, proper financial model needs to be devised to compensate EVs for providing reactive power. This could be based on the economic benefits that utility could achieve by deferring installation of reactive power supporting devices (e.g., cap banks) on the distribution feeders. However, there could also be mandatory regulatory rules (e.g., California Rule 21) to enforce reactive power support from the DERs.

V. Conclusion

This paper first developed detailed high-fidelity model of battery and EV on-board charger that allows four-quadrant operation. The model incorporates SOC dynamics, dynamic of EV current response, and a charge control model with constant current (CC) and constant voltage (CV) charging options, which is a significant improvement over the simplified EV models used in literature which only considers SOC dynamics. The mathematical model of the battery and charger is validated using experimental test data available for Toyota IQ EV. Then, the EV on-board charger model is integrated to a typical North American low voltage distribution feeder to demonstrate the usefulness of four-quadrant dispatch of EVs in supporting voltage on the feeder. For this, voltage regulation signals (in terms of P,Q dispatch of EVs) are generated from an optimal power flow model and the EVs are dispatched accordingly. Our simulation demonstrates effectiveness of dispatching EVs in 4-quadrant for supporting voltage on the distribution feeders.

References

[1] S. Shafiee, M. Fotuhi-Firuzabad, and M. Rastegar, "Investigating the impacts of plug-in hybrid electric vehicles on power distribution systems," *IEEE Trans. Smart Grid*, vol. 4, no. 3, pp. 1351–1360, Sep 2013.

[2] E. Sortomme, M. M. Hindi, S. D. J. MacPherson, and S. S. Venkata, "Coordinated charging of plug-in hybrid electric vehicles to minimize distribution system losses," *IEEE Trans. Smart Grid*, vol. 2, no. 1, pp. 198–205, Mar 2011.

[3] E. Ucer, M. C. Kisacikoglu, and M. Yuksel, "Analysis of an internet-inspired EV charging network in a distribution grid," in *IEEE Transmiss. Distr. Conf.*, Apr 2018.

[4] J. Wang, G. R. Bharati, S. Paudyal, O. Ceylan, B. P. Bhattarai, and K. S. Myers, "Coordinated electric vehicle charging with reactive power support to distribution grids," *IEEE Trans. Ind. Informat.*, pp. 1–1, 2018.

[5] M. J. E. Alam, K. M. Muttaqi, and D. Sutanto, "A controllable local peak-shaving strategy for effective utilization of PEV battery capacity for distribution network support," *IEEE Trans. Ind. Appl.*, vol. 51, no. 3, pp. 2030–2037, 2015.

[6] S. Shao, M. Pipattanasomporn, and S. Rahman, "Demand response as a load shaping tool in an intelligent grid with electric vehicles," *IEEE Trans. Smart Grid*, vol. 2, no. 4, pp. 624–631, Dec 2011.

[7] A. Di Giorgio, F. Liberati, and S. Canale, "Electric vehicles charging control in a smart grid: A model predictive control approach," *Control Engineering Practice*, vol. 22, pp. 147–162, 2014.

[8] W. Kempton and J. Tomić, "Vehicle-to-grid power fundamentals: Calculating capacity and net revenue," *J. of Power Sources*, vol. 144, no. 1, pp. 268–279, 2005.

[9] J. de Hoog, T. Alpcan, M. Brazil, D. A. Thomas, and I. Mareels, "Optimal charging of electric vehicles taking distribution network constraints into account," *IEEE Trans. Power Syst.*, vol. 30, no. 1, pp. 365–375, Jan 2015.

[10] G. R. Bharati and S. Paudyal, "Coordinated control of distribution grid and electric vehicle loads," *Electric Power Systems Research*, vol. 140, pp. 761 – 768, 2016.

[11] K. Clement-Nyns, E. Haesen, and J. Driesen, "The impact of charging plug-in hybrid electric vehicles on a residential distribution grid," *IEEE Trans. Power Syst.*, vol. 25, no. 1, pp. 371–380, Feb 2010.

[12] M. Mojdehi and P. Ghosh, "An On-Demand Compensation Function for an EV as a Reactive Power Service Provider," *IEEE Trans. Veh. Technol.*, vol. 65, no. 6, pp. 4572–4583, Jun 2016.

[13] I. Vittorias, M. Metzger, D. Kunz, M. Gerlich, and G. Bachmaier, "A bidirectional battery charger for electric vehicles with V2G and V2H capability and active and reactive power control," in *Proc. IEEE Transportation Electrification Conference and Expo.*, 2014, pp. 1–6.

[14] M. C. Kisacikoglu, M. Kesler, and L. M. Tolbert, "Single-phase on-board bidirectional PEV charger for V2G reactive power operation," *IEEE Trans. Smart Grid*, vol. 6, no. 2, pp. 767–775, Mar 2015.

[15] M. Kesler, M. C. Kisacikoglu, and L. M. Tolbert, "Vehicle-to-grid reactive power operation using plug-in electric vehicle bidirectional offboard charger," *IEEE Trans. Ind. Electron.*, vol. 61, no. 12, pp. 6778–6784, Dec 2014.

[16] M. C. Kisacikoglu, B. Ozpineci, and L. M. Tolbert, "Examination of a PHEV bidirectional charger system for V2G reactive power compensation," in *Proc. IEEE Applied Power Electronics Conference and Exposition*, 2010, pp. 458–465.

[17] M. A. Azzouz, M. F. Shaaban, and E. F. El-Saadany, "Real-time optimal voltage regulation for distribution networks incorporating high penetration of pevs," *IEEE Trans. Power Syst.*, vol. 30, no. 6, pp. 3234–3245, Nov 2015.

[18] N. Mehboob, M. Restrepo, C. A. Cañizares, C. Rosenberg, and M. Kazerani, "Smart operation of electric vehicles with four-quadrant chargers considering uncertainties," *IEEE Trans. Smart Grid*, pp. 1–1, 2018.

[19] M. Restrepo, C. A. Cañizares, and M. Kazerani, "Three-stage distribution feeder control considering four-quadrant EV chargers," *IEEE Trans. Smart Grid*, vol. 9, no. 4, pp. 3736–3747, Jul 2018.

[20] A. Meintz, T. Markel, M. Jun, and J. Zhang, "Integrating PEVs with renewables and the grid," in *Proc. IEEE Transportation Electrification Conference and Expo.*, 2015.

[21] S. Paudyal, C. Cañizares, and K. Bhattacharya, "Optimal operation of distribution feeders in smart grids," *IEEE Trans. Ind. Electron.*, vol. 58, no. 10, pp. 4495–4503, Oct 2011.

[22] R. Tonkoski, L. A. Lopes, and T. H. El-Fouly, "Coordinated active power curtailment of grid connected pv inverters for overvoltage prevention," *IEEE Trans. Sustainable Energy*, vol. 2, no. 2, pp. 139–147, Apr 2011.

[23] "IEEE standard for interconnection and interoperability of distributed energy resources with associated electric power systems interfaces," *IEEE Std 1547-2018 (Revision of IEEE Std 1547-2003)*, pp. 1–138, April 2018.